

A. KENESBAYEVA¹, Associate Professor, PhD

Kh. M. KASSYMKANOVA¹, Professor, Doctor of Engineering Sciences, *k.kassymkanova@satbayev.university*

A. M. BERMUKHANOVA¹, Candidate for a Doctor's Degree

N. A. MILETENKO², Senior Researcher, Candidate of Engineering Sciences

¹Satbayev University, Almaty, Kazakhstan

²Academician Melnikov Institute of Comprehensive Exploitation of Mineral Resources—IPKON, Russian Academy of Sciences, Moscow, Russia

CREATION OF GRAVIMETRIC MAP AND DEEP STRUCTURE ANALYSIS OF THE TURKISTAN REGION

Introduction

Deeper understanding of the Earth's gravitational field and its time history is necessary for solving a wide range of problems in science and technology, including geophysical exploration of mineral deposits [1, 2], geodynamic research [3–5], climate forecasting [6, 7], as well as shift of poles [8–10] or finding underground sources of heat and water [11, 12].

Gravimetric data help get information about density of rocks, or configuration and depth of such large structures as sedimentary basins, faults, upheavals and downfolds. Gravity anomalies often point at faulted zones, which is important for the evaluation of geodynamic activity and prediction of possible earthquakes in a region. In geodetic measurement and engineering survey, gravimetry allows taking into account geological conditions, for instance, in construction of dams, tunnels, large buildings and infrastructures. Also, gravimetric data are necessary to improve precision of geodetic surveying and map-making, for instance, when building a geodID model or revising coordinates [13, 14].

Kazakhstan possesses a huge collection of gravimetric data from land-based and satellite surveying carried out in different years by geophysical and geological exploration teams.

Since the measurements had different density and accuracy, and were conducted in various topographic conditions, it is required to examine quality of the available gravimetric data and integrate them into a unified basis for the further use in modeling the Earth's gravity field in Kazakhstan, and for solving various geodetic, geophysical and other type problems.

The aim of this study is the comparative analysis of the precision provided by the global geopotential model XGM2019e_2159 and by the gravimetric surveys in the Turkistan Region, and the use of the gravimetric data in mapping of the Bouguer anomalies and for the deep-earth analysis of the test area.

Research area

The Turkistan Region lies in the south of Kazakhstan at the border with Uzbekistan (Fig. 1), inside the areas of deserts and semi-deserts. The land forms are valleys and lowlands. In the east there are branches of the western Tian-Shan, such as the Karatau Mountains which are the source of rivers and other water types. In the west and in the center of the test area, the even deserts and semi-deserts prevail. The regional hydrography is represented by the Syr Darya River and manmade water bodies, including the largest Shardara Reservoir. The problem connected with water resources is topical because of arid climate and high dependence on transboundary rivers. The region possesses many minerals, including phosphorite, building materials and rare metals. Ecologically, the Turkistan Region experiences desertification.

This article describes creation of a gravimetric map for the Turkistan Region in Kazakhstan, to be later on used in solving geological, geophysical and geodetic problems. The gravimetric surveying data on the Turkistan area are to the courtesy of the National Geological Service (NGS JSC). The archival gravimetric maps were scanned, digitized, geographically fixed and systematized. The diagrammatic maps of the area coverage are given with the specified scales and density of surveying. The comparative analysis of the precision of the global geopotential model XGM2019e_2159 is carried out using the land-based and air-borne gravity data on the test area. The map of the Bouguer anomalies is created for the Turkistan Region at a scale of 1:200000, and the gravity field transforms are made using the radially averaged strength spectrum, to determine the regional and residual gravity anomalies and for the further geological characteristic of the Turkistan Region.

Keywords: gravimetric map, gravity anomaly, Bouguer anomaly, Fourier transform, trend analysis, frequency spectrum, transform core

DOI: 10.17580/em.2025.02.09

Methods and materials

Recently, modernization of the national geodetic datum of Kazakhstan is carried out, including the gravimetric reference frame. The previous gravimetric reference of Kazakhstan represented the national gravimetric network (NGN) of class I with 77 points with an accuracy of $\pm 0.03\text{--}0.04$ mGal, class II with 785 points with an accuracy of ± 0.06 mGal, class III with 3500 points with an accuracy of $\pm 0.02\text{--}0.04$ mGal (relative to class I points). Using the gravimetric data over the whole area of Kazakhstan, the gravity anomaly maps were drawn at different times and at different scales of 1:1000000, 1:500000 and 1:200000. For the promising sites, a series of gravity maps was prepared and issued at a scale of 1:50000 (over 100 trapezoids) [15].

The gravimetry of the Turkistan Region was integrated with other geophysical surveying methods towards the precise geological delineation of mineral deposits, comprehensive analysis of rocks and creation of detailed gravity maps of the promising sites. As a result, the test area is entirely covered by gravimetric observations of different scale (Fig. 2).

In the test region, gravity surveys at the scales of 1:10000 and 1:25000 started in the 1970s. In 1982–1986 the works were carried out in the center of the Leontyev depression and Shu-Sarysu basin. Nearly 50% of the test area is embraced by surveying at a scale of 1:50000, commonly used since the mid-1900s, with the peak of application in the 1960–80s. Generally, the surveying was performed by the Central, Turlan and Ural geophysical expeditions, Karatau geological exploration expedition, Kazakhstan aerogeology expedition and by Izdenis JSC.

Approximately 20% of the test area is covered by the scale 1:100000 surveying performed in different periods of time, starting from the mid-1900s and up to the present day, for the regional territorial research, including deep structure, reference networking, etc. These works were implemented by the Turlan geophysical expedition, Tashkentgeologia Integrated Geophysical Exploration Expedition and by GEOKEN Center LLC. The average accuracy of the gravimetric measurements was $\pm 0.03\text{--}0.10$ mGal for the ground elevations of $\pm 0.05\text{--}0.25$ m.

The scale 1:200000 surveys cover a bit less than a half of the test area. The main agencies engaged in the surveys are the Ustyurt party, Neftegeofizika Special Regional Geophysical Expedition, KGGT Aerogeophysical Expedition and GEOKEN Center LLC.

During the research, the fellow workers of the Satbayev University and GEOKEN Center carried out the analysis of gravimetric data and integrated them into a unified data base. An updated gravimetric map at a scale of 1:200000 was created for the whole Turkistan Region. The earlier gravity anomaly maps at the scale of 1:200000 were created for the area of Kazakhstan in the period between 1961 and 2001 using all reliable information of gravimetric surveys performed by that time.

The layout of points belonging in the gravimetric and field reference networks, as well as intermediate observation sites in the test area are shown in **Fig. 3**. The density of the gravimetric points in the test area is uneven, for instance, in the north and in the center, the density is higher, and its decreases closer to the south of the test area. This is explained by the fact that in the north of the Turkistan Region, there are mineral exploration zones, and

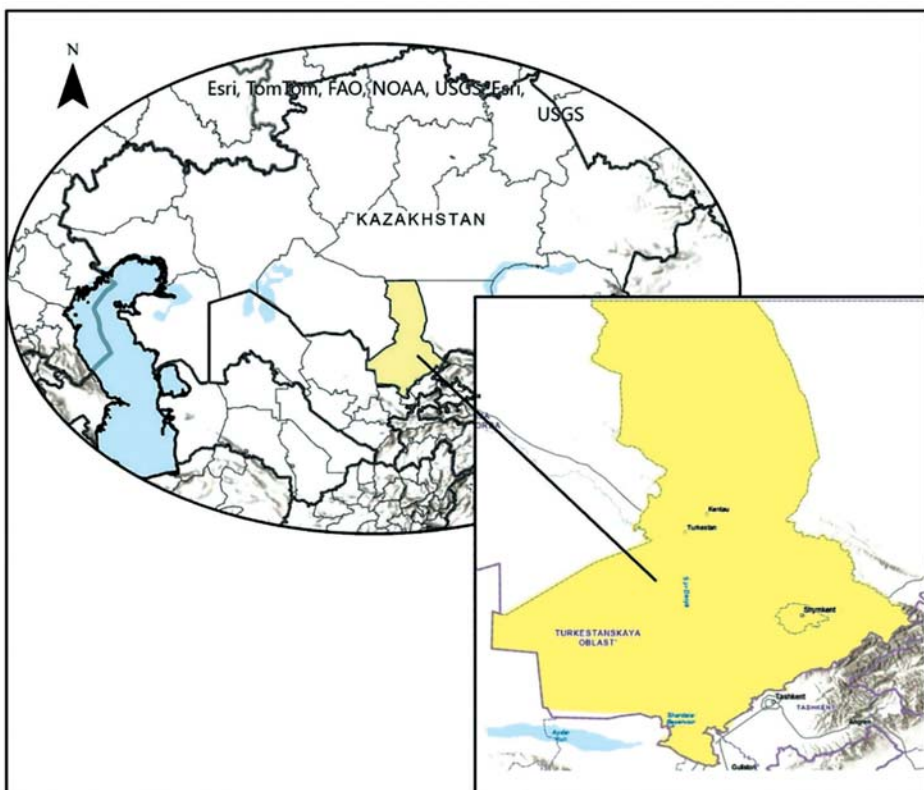


Fig. 1. Location of the Turkistan Region

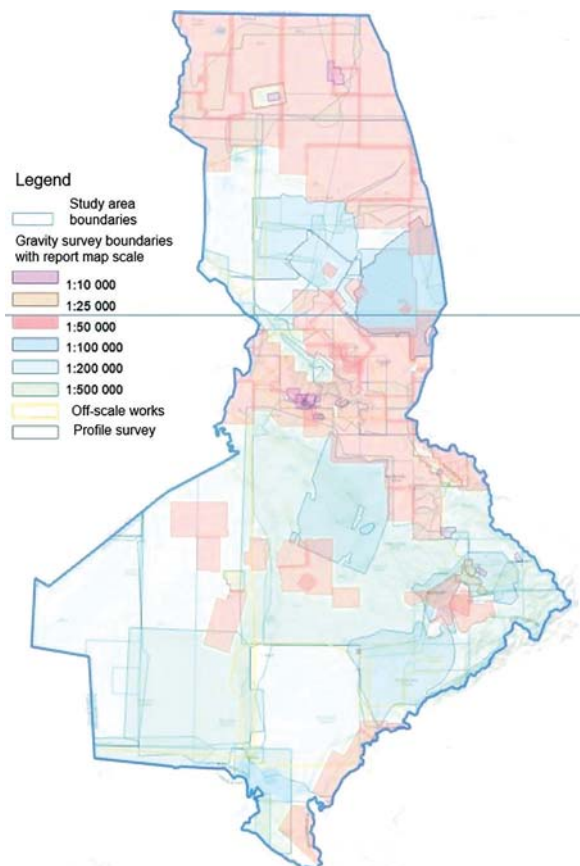


Fig. 2. Gravity survey coverage of the Turkistan area

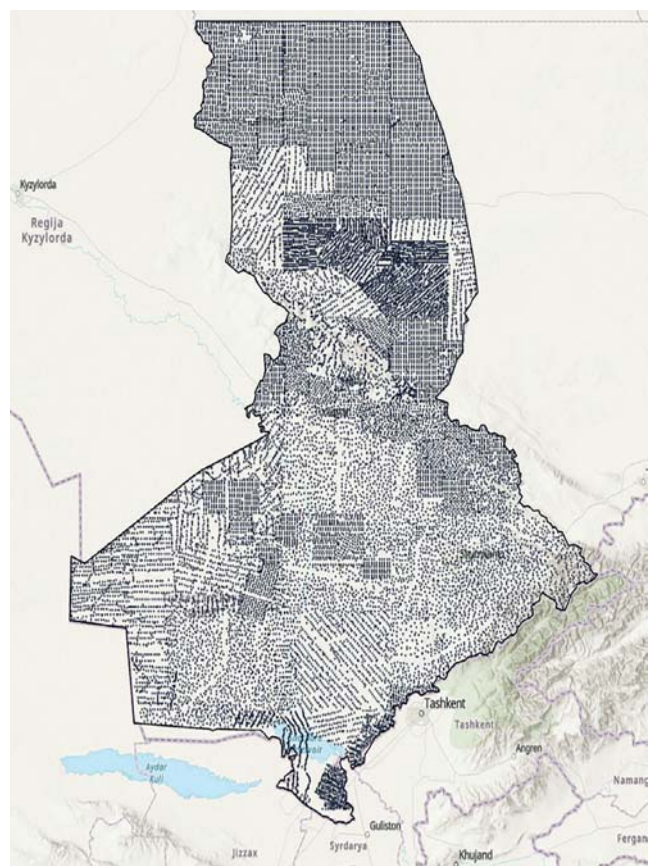


Fig. 3. Layout of gravimetric points

the integrated geophysical research has involved a more comprehensive gravimetric survey here.

Almost all gravimetric surveys at a scale of 1:200000 carried out in the test area were included in preparation of the gravity maps at the scale of 1:200000. Some surveys at a scale of 1:100000 were used in plotting of individual sheets of the map. The surveys implemented in the center and in the south of the test area were discarded because of the early year of surveying.

So, it is possible to state that the published gravimetric maps of the Turkistan Region used mostly the data of surveying at the scales of 1:50000 and 1:200000, which ensured the required precision of the maps. Digitalization of the maps produced an integrated array of quality data from surveying at a scale of 1:200000 and also larger scales.

Analysis of gravimetric data. The land-based gravimetric measurements carried out in the Turkistan Region were compared with the model data calculated using the coefficients of the recent global geopotential model XGM 2019e_2159.

The global geopotential model XGM2019e_2159 became available in 2019 on the website of the German International Center for Global Earth Models (ICGEM) in Potsdam [13]. The model XGM2019e_2159 is a combined geopotential model with its harmonic coefficients which were first determined in terms of spheroidal harmonics and then, to conform with ICGEM standard, were converted to spherical harmonics. On ICGEM's website, the model XGM2019e_2159 is available up to a spherical harmonic's degree $N = 2190$ [16].

The gravity anomaly Δg is determined using the data of the geopotential model XGM2019e_2159 from the formula [17]:

$$\Delta g = \gamma \sum_{n=2}^N (n-1) * \sum_{m=0}^n (\Delta \bar{C}_{nm} \cos m\lambda + \bar{S}_{nm} \sin m\lambda) \bar{P}_{nm}(\sin \varphi), \quad (1)$$

where γ is the normal gravity; n and m are the degree and order of a spherical harmonic; $\Delta \bar{C}_{nm}$ is the difference of standardized cosine geopotential coefficients; \bar{S}_{nm} is the standardized sine geopotential coefficient; λ and φ are the longitude and latitude of a point; N is the spherical harmonic's degree; $\bar{P}_{nm}(\sin \varphi)$ are the standardized associated Legendre functions.

The comparison of the gravity anomalies from the land-based gravimetric measurements and from the modeling data uses the formula [18]:

$$\delta \Delta g(P) = \Delta g_H(P) - \Delta g_{\text{mod}}(P), \quad (2)$$

where $\Delta g_H(P)$ are the gravity anomalies calculated using the gravimetric measurements at the point $P(\varphi, \lambda)$ on ground surface; $\Delta g_{\text{mod}}(P)$ are the gravity anomalies at the same point from the data of the model XGM2019e_2159.

Deep subsurface investigation. The gravity field represents distribution of equivalent density nonuniformities of gravitational masses conditionally 'brought' to an equipotential surface and, therefore, provides no answer to the question at which specific depths these masses are located.

For referencing structural nonuniformities at different depths, various methods of transformation of the initial anomaly field are used, which 'aggravate' either regional or local anomalies.

The most common approaches are the analytical extensions of the field to the upper or lower half-spaces, which allows identifying various components of the gravity fields. The upward recalculations, i.e., to the levels above the observation surface, lead to a drop in the amplitudes of the local anomalies and to a slight change in the regional anomalies. This makes it possible, at an optimal selected height of the recalculations, to match the transformed anomalies and the regional background [19].

One of the most efficient methods of disintegrating a complex field is the analytical extension to the upper half-space—the recalculations at a certain height h . The field recalculated in the upper half-space preserves mostly anomalies governed by large deep-seated geological bodies and by density

interfaces at great depths. The effects conditioned by shallow and small objects get mostly suppressed [20].

The downward recalculation of the field, below the observation plane, similarly to the calculation of higher derivatives of gravity force, leads to highlighting of local anomalies. Using the maps and graphs of the observed (Δg_{obs}) or local (Δg_{loc}) and regional (Δg_{reg}) gravity anomalies, it is possible to draw the quality conclusions on the density nonuniformities which condition these anomalies. The positive anomalies point at the location of denser rocks as compared with the enclosing rock mass, the negative anomalies agree with the location of less dense rocks, or with upheaval or sinking of a subhorizontal interface of different density rocks. The zones of the increased horizontal gradients conform with the steep interfaces of different density rocks.

Fourier transforms. For the case of land-based gravimetric surveys, the Fourier transform is carried out using the formulas below [20]:

$$f(x, y) = \frac{1}{2\pi} \int \int_{-\infty}^{\infty} S(\omega_1, \omega_2) e^{i(\omega_1 x + \omega_2 y)} d\omega_1 d\omega_2, \quad (3)$$

$$S(\omega_1, \omega_2) = \frac{1}{2\pi} \int \int_{-\infty}^{\infty} f(x, y) (\omega_1, \omega_2) e^{i(\omega_1 x + \omega_2 y)} d\omega_1 d\omega_2, \quad (4)$$

where $\omega_1 = \frac{2\pi nx}{b-a}$ and $\omega_2 = \frac{2\pi ny}{d-c}$ are the spatial frequencies; i is an imaginary number; $(b-a)$ and $(d-c)$ are the sizes of the survey area along the axes OX and OY, respectively; $S(\omega_1, \omega_2)$ is the amplitude-frequency spectrum of the function $f(x, y)$.

The calculation of the spectrum of the field transform $f(x, y)$ needs finding a product of two spectra [20]:

$$S_v(\omega_1, \omega_2) = S(\omega_1, \omega_2) \Phi(\omega_1, \omega_2), \quad (5)$$

where $S_v(\omega_1, \omega_2)$ is the transform spectrum; $\Phi(\omega_1, \omega_2)$ is the spectral characteristic of the gravity field recalculations at the height h and is generally expressed as: $\Phi(\omega) = e^{-\omega h}$.

The radially averaged spectrum of the gravity field strength allows representing the gravity field strength as a function of the spatial frequency (wavenumber) averaged along a direction in the space of frequencies.

The radially averaged strength spectrum $P(k)$ is expressed in terms of 2D gravity field Fourier transform $\Phi(x, y)$:

$$P(k) = \frac{1}{N_k} \sum_{k=k+\Delta k/2}^{k+\Delta k/2} |\Phi(k_x, k_y)|^2,$$

where $\Phi(k_x, k_y)$ is the Fourier spectrum of gravity field; $k = \sqrt{k_x^2 + k_y^2}$ the wavenumber; N_k is the number of points in the circular interval $\left[k - \frac{\Delta k}{2}, k + \frac{\Delta k}{2} \right]$; Δk is the width of the circular interval of averaging, which defines the thickness of a circle in the frequency domain, in which the spectrum values are averaged.

Results

For the comparison of the land-based gravimetric measurements in the Turkistan Region and the calculations from the data of the global geopotential model XGM2019e_2159, 320 reference points were selected in the gravimetric networks of classes I–III, and the gravity force values were determined at that points at an error from ± 0.02 to ± 0.06 mGal. The layout of the reference gravimetric points in the test area and the results of the compared gravity anomalies from the land-based gravimetric measurement and from the global geopotential model are depicted in **Fig. 4**.

The density of the reference points is comparatively uniform in the test area, except for its north-east where this density is somewhat higher, due to the more detailed gravimetric surveys carried out here during exploration of mineral deposits which occur in this area.

The analysis of the difference field in Fig. 4 allows drawing the following conclusions: the difference between the gravity anomalies calculated using the global geopotential model XGM 2019e_2159 and the land-based measurements has the maximum values in the south of the test area and in a small site in the middle, which is most probably caused by a low accuracy of the geopotential model due to lack of the land data; the mean square error of the land-based and model gravimetric data difference is -16.8 mGal in a range from $+37$ to -50 mGal.

Deep subsurface investigation. As a result of the calculation of the radially averaged strength spectrum, which is a function of the wavenumber and is calculated as averaging of energies of the same wavenumber in all directions, the maps of the regional anomaly field and the residual anomaly field are obtained (Fig. 5).

The negative gravity anomalies are observed across the whole test area. As seen in Fig. 5, the gravity anomalies in the north vary in a range from -20 to -86 mGal, which probably conforms with the Shu-Sarysu depression representing an Epicalledonian basin with a two-layer structure of the sedimentary cover. The intensity and shapes of the anomalies can be caused by the differences in the thickness of the sedimentary cover, in the structure of the basement, and by the presence of the deep-seated faults. The low values of the gravity anomalies may be connected with the deeper sites of the depression, and the smaller anomalies can be connected with the thinner sedimentary cover or with the upheaved basement. This may point at the local upheaval or platform projections of the basement inside the basin. The lower level of this basin is composed of the Paleozoic

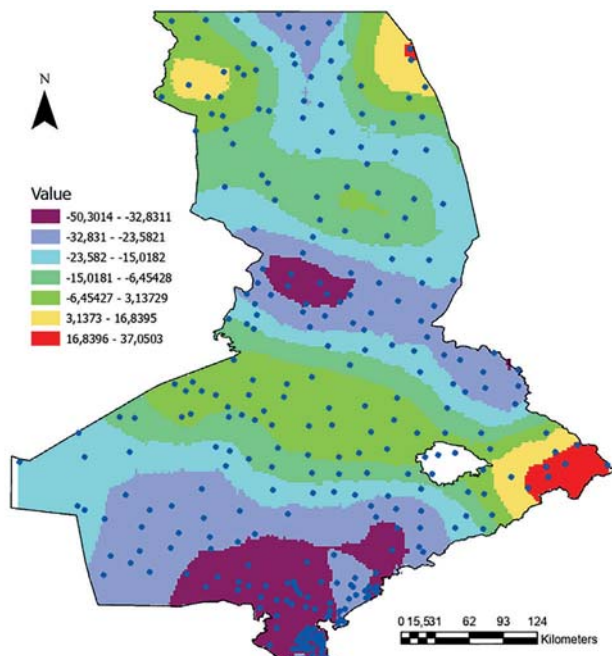


Fig. 4. Differences of the field from the gravimetric surveying and geopotential model XGM 2019e_2159

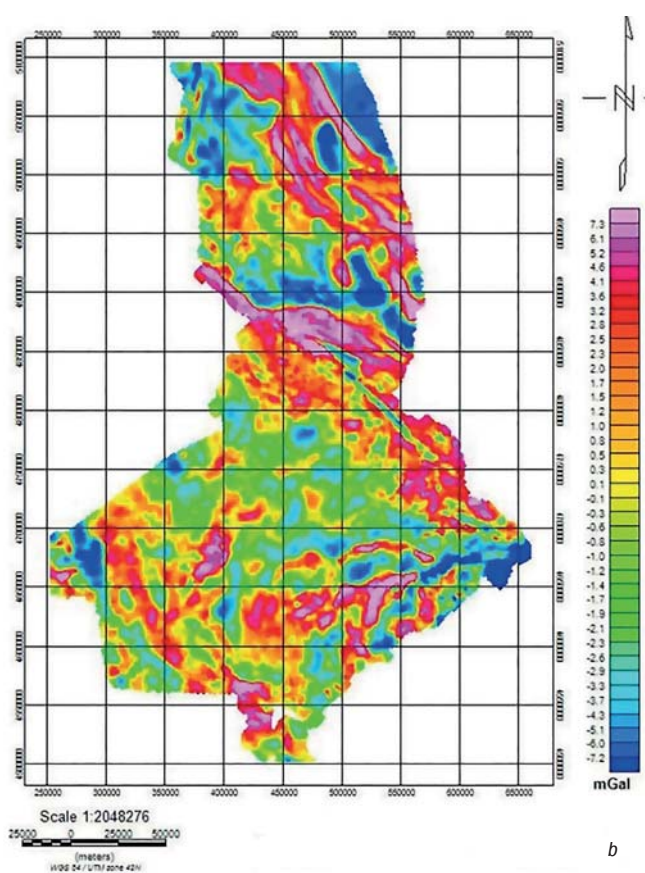
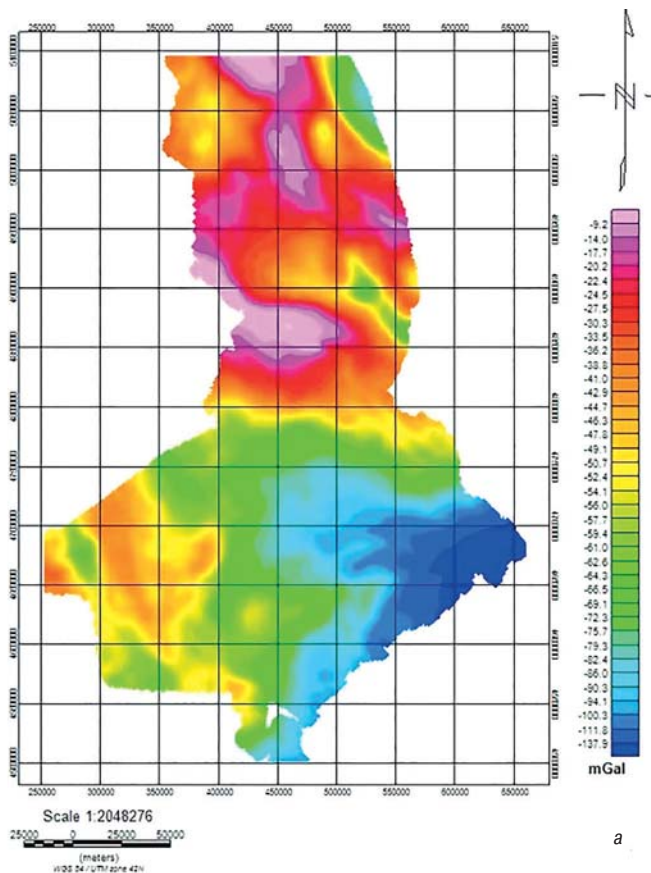


Fig. 5. Maps of regional and residual gravity anomalies:
a – regional gravity anomalies; b – residual gravity anomalies

moderately dislocated lithified rocks at the depths of 700–1000 m, and the upper level—of the Mesozoic–Cenozoic flat platform mantle of the Cretaceous and Cenozoic sandy–clayey sediments. The bottom of the mantle is composed of speckled clay of the Low-Cretaceous and Cenomanian age [21].

In the south of the test area, the gravity anomalies range from –45 to –138 mGal and can be connected with the Syr Darya intracontinental basin. In the Shymkent-adjacent region of this basin, by geological and geophysical data, near the northeastern corner, there are the largest northwestward Near-Karatau and Turkistan faults. In the rest of the region, there are the northeastward and, to a lesser degree, northwestward faults. According to gravity surveys, some rock formations overlaid with the Mesozoic–Cenozoic to Paleozoic soft sediments up to 1600–1800 m thick occur in a semi-circle and are the northern and eastern half of the giant Irsu–Urtabas ring structure. The controlling faults have an evident relation to the top mantle of the Earth's crust. All this can be an explanation of the local negative gravity anomalies in the north of the region being discussed.

The analysis of the map of the residual gravity anomalies proves a probable connection of the revealed anomalies with the presence of the iron ore, aluminum and copper–iron ore deposits. The latter, as a rule, adjoin the edges of the Syr Darya basin and the higher order tectonic structures as well. In these zones, the outcrops or subsurface sediments of the Devonian–Carboniferous period are detected, which are greatly complicated by a system of overthrusts and faults of different orientation and thickness, supposedly genetically related with multi-phase and different-age intrusive formations.

Conclusions

The developed map of the Bouguer anomalies for the area of the Turkistan Region meets the modern standards of precision and ensures the detailed and reliable characteristic of the regional gravity field. The comparison of the obtained values with the model anomalies from the global geopotential model demonstrates the advantage of the developed map in terms of the spatial resolution and accurate mapping of the local and regional peculiarities of the gravity field.

The implemented transformations of the gravity field made it possible to push the interpretation limits of the map. As a result, we acquired additional knowledge of the deep structure of the Earth's crust and identified the anomalous zones potentially related with various geological structures and processes.

In the long term, the presented gravimetric map is usable in solving a wide range of theoretical and applied problems, including the geological and structural zoning, prediction and exploration of mineral resources, geodynamic activity assessment, as well as the investigation of potential localization of heat sources and aquifers.

Acknowledgments

This research is funded by the Committee of Science of the Ministry of Science and Higher Education of the Republic of Kazakhstan (Grant No. BR21882366 «Development of a geoid model of the Republic of Kazakhstan as the basis of a unified state coordinate system and heights»).

References

1. Chipanta N., Lubilo F., Nyimbili P. et al. Application of GOCE satellite gravimetric data for mineral exploration. *Zambia ICT Journal*. 2023. Vol. 7(1). pp. 1–6.
2. Guglielmetti L., Moscariello A. On the use of gravity data in delineating geologic features of interest for geothermal exploration in the Geneva Basin (Switzerland): Prospects and limitations. *Swiss Journal of Geosciences*. 2021. Vol. 114, No. 15. DOI: 10.1186/s00015-021-00392-8
3. Zanutt A., Negusini M., Vittuari L. et al. New geodetic and gravimetric maps to infer geodynamics of Antarctica with insights on Victoria Land. *Remote Sensing*. 2018. Vol. 10, Iss. 10. ID 1608.
4. Sun H., Cui X., Xu J. et al. Progress of research on the Earth's gravity tides and its application in geodynamics in China. *Pure and Applied Geophysics*. 2022. DOI: 10.1007/s00024-022-03060-6
5. Oliveira dos Santos A., Mohriak W., Costa Dutra A., Costa dos Santos A. Geophysical characterization and 2D gravimetric modeling: Application to tectonic control of the Vitoria-Trindade Ridge (Vtr-Es, Brazil). *Journal of South American Earth Sciences*. 2024. DOI: 10.2139/ssrn.4821864
6. Robinson E. L., Clark D. B. Using gravity recovery and climate experiment data to derive corrections to precipitation data sets and improve modelled snow mass at high latitudes. *Hydrology and Earth System Sciences*. 2020. Vol. 24. pp. 1763–1779.
7. Tapley B. D., Watkins M. M., Flechtner F. et al. Contributions of GRACE to understanding climate change. *Nature Climate Change*. 2019. Vol. 9. pp. 358–369.
8. Andreev A. O., Demina N. Y., Zagidullin A. A. et al. Analysis of topocentric and gravimetric data from modern space missions. *Journal of Physics: Conference Series*. 2018. Vol. 1135. ID 012002.
9. Jianli Chen. Satellite gravimetry and mass transport in the earth system. *Geodesy and Geodynamics*. 2019. Vol. 10, Iss. 5. pp. 402–415.
10. Seoane L., Nastula J., Bizouard C., Gambis D. The use of gravimetric data from GRACE mission in the understanding of polar motion variations, *Geophysical Journal International*. 2009. Vol. 178, Iss. 2. pp. 614–622.
11. Odero E., Githiri J., K'Orrowe M. Exploring heat sources using gravimetric data: A case study of Magadi Geothermal Prospect, Kenya. *Journal of Geoscience and Environment Protection*. 2024. Vol. 12, No. 5. pp. 147–161.
12. Landon J. S. H. Improving groundwater storage change estimates using time-lapse gravimetry with Gravi4GW. *Environmental Modelling & Software*. 2022. Vol. 150. ID 105340.
13. Abbak R. A., Sjöberg L. E., Ellmann A., Ustun A. A precise gravimetric geoid model in a mountainous area with scarce gravity data: A case study in central Turkey. *Studia Geophysica et Geodaetica*. 2012. Vol. 56. pp. 909–927.
14. Jiang T., Dang Y., Zhang C. Gravimetric geoid modeling from the combination of satellite gravity model, terrestrial and airborne gravity data: A case study in the mountainous area, Colorado. *Earth Planets and Space*. 2020. Vol. 72, No. 189. DOI: 10.1186/s40623-020-01287-y
15. Kassymkhanova Kh. M., Kenesbayeva A., Orynbassarova E. O., Zhanakulova K. A., Adebyet B. Preparing the gravimetric base to create a geoid model of Kazakhstan. *Bulletin of D. Serikbayev EKTU*. 2024. No 3. pp. 62–73.
16. Ganagina I. G., Kobeleva N. N., Goldobin D. N., Zverev I. V. Gravimetric knowledge analysis of the Novosibirsk region territory according to ground measurements data. *Vestnik SSU GT*. 2022. Vol. 27, No. 6. pp. 5–14.
17. Kanushin V. F., Karpik A. P., Ganagina I. G. et al. Research of modern global models of the Earth's gravitational field: Monograph. Novosibirsk : SGUGIT, 2015. 270 p.
18. Kanushin V. F., Ganagina I. G., Goldobin D. N. et al. Comparison of the GOCE project satellite models with different sets of independent terrestrial gravimetry data. *Vestnik SSU GT*. 2014. Vol. 3, No. 27. pp. 21–34.
19. Issagaliyeva A. K., Isayev V. I., Istejkova S. A. Methodology of gravimetric data interpretation in the construction of a geological model of the Caspian region's crust. *Herald of the Kazakh-British Technical University*. 2020. Vol. 17, No. 2. pp. 21–29.
20. Dolgal A. S. Gravimetry and magnetometry: Transformations of geopotential fields: a tutorial. Perm : PGNIU, 2022. 140 p.
21. Akylbekov S. A., Alniyazov G. U., Uzhenkov B. S. Prospects of the Atameken (Shymkent–Turkistan) ore region in search of new deposits of solid minerals. *Geology and Subsoil Protection*. 2022. No. 4(85). pp. 4–32. [EM](#)